2-25-2014

Linear and Nonlinear Motion of a Barotropic Vortex

Israel Gonzalez
igonz008@fiu.edu

DOI: 10.25148/etd.FI14040853

FLORIDA INTERNATIONAL UNIVERSITY

Miami, Florida

LINEAR AND NONLINEAR MOTION OF A BAROTROPIC VORTEX

A thesis submitted in partial fulfillment of

requirements for the degree of

MASTER OF SCIENCE

in

GEOSCIENCES

by

Israel Gonzalez III

2014

To: Dean Kenneth G. Furton
College of Arts and Sciences

This thesis, written by Israel Gonzalez III, and entitled Linear and Nonlinear Motion of a Barotropic Vortex, having been approved in respect to style and intellectual content, is referred to you for judgment.

We have read this thesis and recommend that it be approved.

_____
Ping Zhu

_____
Robert Burgman

_____
Hugh E. Willoughby, Major Professor

Date of Defense: February 25, 2014

The thesis of Israel Gonzalez III is approved.

_____
Dean Kenneth G. Furton
College of Arts and Sciences

_____
Dean Lakshmi N. Reddi
University Graduate School

Florida International University, 2014

ACKNOWLEDGMENTS

I would like to acknowledge the National Science Foundation for funding the project (AGS-1211172). A special thank you goes to my major advisor, Professor Hugh E. Willoughby for his support, guidance, and tutelage as well as schematics from his MET4532 course for the first five figures in my thesis. I am also grateful for his efforts in writing outstanding proposals for the project to get funded. He has been instrumental in my progression as a meteorology student. Collaborating with him was a rewarding experience and it is a pleasure to call him my friend and colleague. My remaining committee members, Professors Ping Zhu and Robert Burgman also deserve my gratitude for their assistance and feedback. Lastly, I want to acknowledge my family because their love, encouragement, and jubilation over me earning a Master's Degree is a reminder of how fortunate I truly am.

ABSTRACT OF THE THESIS

LINEAR AND NONLINEAR MOTION OF A BAROTROPIC VORTEX

by

Israel Gonzalez III

Florida International University, 2014

Miami, Florida

Professor Hugh E. Willoughby, Major Professor

The linear Barotropic Non-Divergent simulation of a vortex on a beta plane is consistent with Willoughby's earlier shallow-water divergent results in that it produced an unbounded accelerating westward and poleward motion without an asymptotic limit. However, Montgomery's work which yielded finite linear drift speeds for his completely cyclonic vortex was inconsistent with ours. The nonlinearly-forced streamfunction exhibited a beta-gyre like structure, but with opposite polarity phase to the linear gyres. Utilization of the linear model with time-dependent, but otherwise beta-like, forcing revealed increasing magnitude and phase reversal in the neighborhood of a low cyclonic frequency. Here, the mean bounded vortex has an outer waveguide that supports Vortex Rossby Wave propagation that is faster than the mean flow and confined to a very narrow band of frequencies between zero and the Vortex Rossby Wave cutoff. The low frequency waves constitute the beta-gyre mode described previously by Willoughby.

TABLE OF CONTENTS

LIST OF FIGURES

SYMBOLS

Azimuth angle	λ
Complex streamfunction amplitude	Ψ
Depth/Height	H
Dissipation	K
Doppler-shifted frequency/Angular velocity	Ω
Frequency (apparent)	ω
Geopotential	ϕ
Inertial parameter	ξ_0
Latitude	φ
Length	L
Mean-flow vorticity	ζ_0
Planetary vorticity (Coriolis parameter)	f
Radial wavelength	L_r
Radial wavenumber	k_r
Radial wind component	u
Radial vortex speed	c_r
Radius	r
Relative vorticity	ζ
Streamfunction	ψ
Tangential wavenumber	n
Tangential wind component	v

Tangential vortex speed	c_λ
Time	t
Vortex translation speed	C

ABBREVIATIONS AND ACRONYMS

Asymmetric Balance	AB
Barotropic Non-Divergent	BND
Northeast	NE
North-northeast	NNE
Northwest	NW
Radius of Maximum Wind	RMW
Southeast	SE
South-southwest	SSW
Southwest	SW
Tropical Cyclone	TC
Vortex Rossby Wave	VRW
Wavenumber	WN

INTRODUCTION

Tropical cyclone track forecasting has improved substantially since the mid-20th century, largely through improved understanding of cyclone motion dynamics. The beta (β) gyres are a generally accepted mechanism that contributes to propagation observed in real-life storms. In the 1980s and 1990s, β-gyre dynamics was the focus of intense modeling and observational efforts (e.g., Chan, Holland, Williams, Wang). Semispectral shallow-water barotropic (i.e., no vertical wind shear) linear and nonlinear time-marching models have been utilized by Willoughby (1992, 1994) to simulate vortex motion on a β-plane. The vortex accelerated toward the northwest (NW) without limit, ostensibly through resonant growth of a free linear mode. In the analogous nonlinear model, wave-wave interaction limited the westward and poleward motion to reasonable speeds of 1-2 ms^{-1}. Subsequent work by Montgomery et al. (1997) was unable to replicate the linear result. Here, we revisit the problem in a Barotropic Non-Divergent context both to resolve the question of the free mode's existence and to clarify the nonlinear dynamics. The results elucidate the physics of tropical cyclone motion and may provide a basis for semi-spectral forecast models.

TROPICAL CYCLONES

Rotational Dynamics

Tropical Cyclones (TCs) are diabatically maintained low-pressure systems that draw their energy from the tropical ocean. Their winds swirl counter-clockwise in the Northern Hemisphere around the center in gradient balance with their almost circular pressure field (Figure 1). The pressure-gradient force (blue arrow) points inward toward the low-pressure center and balanced by the outward centrifugal and Coriolis force (green arrow). The opposite is true for high-pressure systems such as anticyclones. The Coriolis Effect is the deflection of a large-scale motion to the right because of the Earth's rotation and as such, acts orthogonally to the right of the wind (black arrow) in the Northern Hemisphere, thereby explaining the flow pattern.

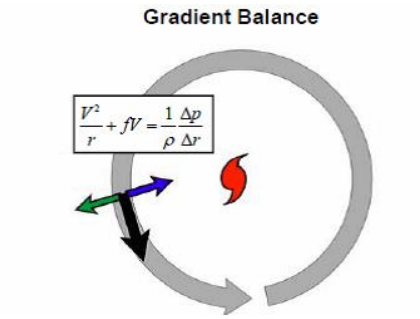

Figure 1. Circular vortex in gradient balance

Vorticity

Since TCs are overwhelmingly rotational, vorticity (e.g., Holton 19, pp.92) is an essential concept to understanding their dynamics. In qualitative terms, vorticity is the measure of rotation separated into two primary parts and defined mathematically as $\nabla \times \vec{v}$ or the curl of the horizontal wind vector $\vec{v}$. Relative vorticity, ζ, is relative to the Earth and characterized as either positive (i.e., cyclonic) or negative (i.e., anticyclonic) rotation;

TCs have positive ζ at their core. The second part is proportional to the vertical component of the Earth's rotation and is known as planetary vorticity, *f*, or the Coriolis parameter. Mathematically, $f=2\Omega\sin\varphi$, where Ω is the angular velocity of the planet and φ is the latitude. Thus *f* is zero at the equator and increases poleward. The spatial gradient of planetary vorticity, $\beta=\partial f/\partial y$, accounts for the β-effect, the change in *f* across the circulation. Additionally, absolute vorticity is the sum of relative and planetary and vorticity. In TCs, the relative vorticity gradient decreases outward from the storm, negative near the center, and becomes less negative outward. In a bounded vortex where circulation approaches zero at large radius, the relative vorticity and its gradient become weakly positive at the periphery.

Vorticity is a conservative property in a Barotropic Non-Divergent (BND), frictionless flow, where it cannot be created nor destroyed. However, in the real atmosphere, (but not in BND flows) it can be stretched or compressed vertically. Tropical Cyclones obtain their energy from the warm ocean surface as convergence of the air swirls into the center. The water evaporates into vapor that rises in the eyewall convection. The vapor then condenses into liquid water and releases latent heat. As a result, TCs have warm cores where rising motion stretches the vorticity upward thus concentrating it and causing the swirling wind to increase. Consequently, the eyewall is where the convection and strongest winds are found. Conversely, sinking motion occurs

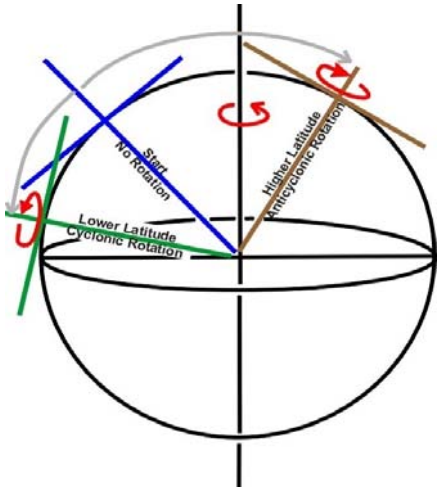

Figure 2. Conservation of absolute vorticity of a nonrotating air parcel

in the eye of the storm which causes the vorticity to compress downward. As a result, the eye is the calmest part of a TC.

In the BND context, absolute vorticity conservation states that if a parcel of nonrotating air at some arbitrary latitude is displaced poleward, f will increase and ζ decrease to retain the same absolute vorticity that it had at its initial position. The air consequently acquires anticyclonic relative vorticity. The opposite is true if that same air parcel was displaced equatorward. The process in Figure 2 occurs in TCs because of their large size and is responsible for formation of asymmetries called the β-gyres.

Structure

The typical structure of a mature TC consists of a well-defined, fairly symmetric circulation with a large outflow pattern near the tropopause (e.g., H~12 km). The low-level circulation is masked by higher convective clouds known as the Central Dense Overcast with an often cloud-free eye. Spiral rain bands of convection wrap around the storm in most, if not all of the quadrants. The secondary circulation induced by latent heat release maintains the storm for times much longer than the orbital period of air swirling around the center. Without it, the vortex would experience rapid spin-down and dissipation.

General Motion

Tropical Cyclones can be thought of as rotating cylinders whose horizontal dimensions (e.g., L~300-2000 km) are an approximate order of 100 times greater than its vertical dimensions (e.g., H~10-12 km). Thus, they fall near the lower margin of the

synoptic scale (i.e., H/L << 1) weather systems. Despite their large size however, they are embedded in the Earth's tropospheric planetary scale flow in which horizontal dimensions are much larger. As a result, TCs are, to a first approximation, blobs of vorticity that move with environmental currents. In the North Atlantic tropics and subtropics (i.e., between 0^0 N and 30^0 N), observations generally show a westward and poleward motion to the right of the background flow, consistent with the easterly (i.e., east to west) flow of the Trade Winds and the southern periphery of the Bermuda and Azores High. When TCs reach the mid-latitudes (i.e., > 30^0 N), their motion is dominated by the stronger prevailing westerlies which are primarily responsible for recurvature out to the cold open North Atlantic. The role of environmental flow in TC motion is evident, but there are other important factors.

In actuality, TC motion is primarily controlled by the winds at mid-levels (i.e., 500 millibars) of the atmospheric environment. In a uniform flow, the steering current would push the TC's vorticity downstream, thus causing it to move with the flow (Figure 3). In addition to their advection by the surrounding "steering currents", TCs also propagate as a result of flow across their centers induced by asymmetries stemming from the β-effect.

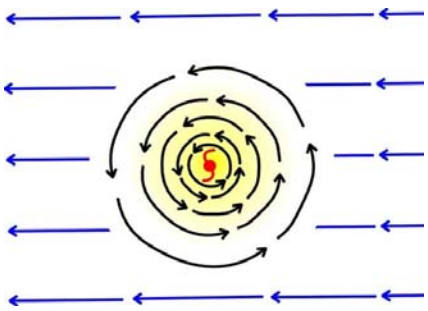

Figure 3. TC embedded in an easterly uniform flow with no vorticity

PREVIOUS WORKS

Vortex Motion on a Beta Plane

Tropical Cyclones move generally with the environmental current but are often observed to deviate slightly from their expected track. A plausible explanation for the deviation is that the stronger Coriolis force exerted on the poleward part of a storm causes it to move to higher latitude, as first suggested by Rossby (1948). He claimed that a net force must exist to drive a TC poleward. Subsequent research in the late 1950s and 1960s seemed to validate the β-effect, but a physical mechanism was not understood until the early 1980s (Chan & Holland). The idea was that the swirling flow of a TC advects *f* within the storm itself and produces two oppositely rotating gyres (called β-gyres) on the periphery, such that the counter flow between them moves northwestward across the center of the vortex. The resulting asymmetric secondary circulation drives the TC poleward and westward and appears responsible for the tendency to move differently from what the environmental steering flow would otherwise dictate.

The linear argument mentioned earlier however was shown to be somewhat inaccurate by Chan & Williams (1987) in terms of explaining the β-effect. From a numerical standpoint, the linear solution of the barotropic vorticity equation in an environment devoid of any steering flow would produce a westward moving vortex with slow propagation. Therefore, nonlinear interactions between the mean vortex swirling flow and *f* must play a significant role in moving the storm poleward. Consequently, scientists became motivated to include nonlinearity in their models to represent vortex motion on a β-plane more realistically.

Beta Gyre Normal Mode Theory

Willoughby (1992, 1994) developed a shallow-water (i.e., H=500 m) divergent, barotropic, time-marching model to simulate both linear and nonlinear vortex motion with a 4 km horizontal resolution on a domain that extended from the center to 3000 km radius. The vortex was bounded in a sense that the circulation approached zero at some large but finite radius thus requiring anticyclonic vorticity and a reversal of vorticity gradient at the vortex periphery from the Circulation Theorem. In his model, the vortex supported two linear normal modes: a neutral normal mode near zero frequency (equivalent to the β-gyre asymmetries), and an alternative vortex with zero relative angular momentum; it had a barotropically unstable mode that exhibited a paired "trailing spiral" asymmetry close to the center.

The linear case produced β-gyre streamfunction dipoles with opposite polarity on either side of the vortex. The asymmetries appeared to represent normal modes of the linear system. A normal mode is defined as a set of parts of an oscillating system in which they obtain a sinusoidal motion at the same frequency (i.e., resonance). When a normal mode is forced at its resonant frequency in the absence of dissipation, it grows linearly with time to large amplitude and known to persist for long periods of time in the absence of forcing. The track from linear calculations showed an essentially constant acceleration poleward and westward to non-physically high speeds. Hypothetically a resonant excitation of near-zero-frequency normal mode by the β-effect appeared responsible.

Willoughby attempted to validate his hypothesis by "switching off" the β-forcing at 240 hrs after the gyres have already established themselves as asymmetric structures.

He then ran the model for an additional 10 days (i.e., to 480 hrs) and found that the asymmetries retained their structure and the near-constant NW track persisted with nearly constant speed on an *f*-plane (where *f* does not vary with latitude). Furthermore, he was able to manipulate the β-gyres by rotating and scaling them to produce any desired initial motion which seemed to support the normal mode theory (Willoughby 1995). Willoughby concluded that a general property of barotropic vortices is the existence of a neutral mode under the condition that the mean vortex is bounded at some finite radius where the circulation is zero.

The analogous nonlinear case considered wave-wave interactions that change the axially symmetric structure of the vortex and limit its speed. In addition, they support wave energy cascade to higher wavenumbers. The interaction with the mean vortex produced an annulus of anticyclonic flow on the vortex periphery that contained a new set of β-gyres but of opposite polarity to the original ones in the linear model.

Asymmetric Balance

Shapiro and Montgomery (1993) developed the Asymmetric Balance (AB) equations for asymmetric motions on circular vortices and applied them to vortex motion on a β-plane in fixed coordinates (1997). Asymmetric Balance allows one to separate the linear and nonlinear balance contributions to the vortex motion when the standard Rossby number (i.e., v_0/fL) is not small. The mathematical framework for studying the slow evolution of rapidly rotating fluid systems such as TCs and addresses asymmetric dynamics that include: spiral rain bands, track, and environmental interaction is what AB represents. Montgomery's somewhat different approach to Willoughby (1992) yielded

inconsistent linear results that produced a vortex speed that asymptoted after 240 hrs at ~6 ms^{-1}. The track was faster than full-physics models or observations and not much slower than Willoughby's linear results (i.e., 8 ms^{-1}) after 240 hrs. Asymmetric Balance requires that the linearized Lagrangian derivative yields frequencies well below the inertia frequency and is not met for low-frequency wavenumber-one perturbations in the vortex core. The vorticity dynamics of their completely cyclonic vortex differ significantly from those of a bounded vortex whose circulation approaches zero at large radius, dissipative (i.e., K=60 m^2s^{-1}) nature of the model, and different vortex tracking method may explain the asymptotic motion. Nevertheless, Montgomery argued against the β-gyre normal mode theory because his results suggest that finite drift speeds are always attained in a vortex with finite depth (i.e., divergent). Moreover, he performed his own set of reinitialization experiments for different types of vortices and found that the β-gyres persisted for long times but not infinitely. The asymmetries decayed with a half time proportional to the radial shear and "axisymmetrized".

SECONDARY CIRCULATION EFFECT ON MOTION

Beta Gyres

Vorticity advection by the surrounding "steering current" is the dominant process in TC motion on an *f*-plane causing simple movement with the background flow in an environment with no vorticity gradients. On the other hand, vorticity advection by the mean swirling flow associated with the vortex dominates in still surroundings on a β-plane (where *f* varies with latitude). From conservation of absolute vorticity, ζ must decrease (as *f* increases) to the north and increase (as *f* decreases) to the south of the TC. The change in ζ is a function only of the storm latitude and the size of the radius of circulation (Marks, 1992). As a result, vorticity pattern of opposite phase forms (anticyclonic to the north and cyclonic on the south) such that there is a beta-induced secondary easterly flow across the vortex. The radial ventilation flow advects cyclonic relative vorticity out of the vortex core on the west side of the center to spin up a cyclonic circulation there. Conversely, inflow on the east brings low relative vorticity into the vortex, spinning up an anticyclonic gyre there. The superposition of the beta-induced and ventilation-induced gyres produces a northeast-southwest (NE-SW) oriented β-gyre streamfunction dipole such that the southeasterly flow between the gyres advects the vortex poleward and westward as shown in Figure 4 (Chan & Williams).

Beta Drift

Tropical Cyclones therefore have two forms of secondary flow that are combined to produce a deviated displacement to the NW irrespective of advection by the large-scale

flow. Vortex-following models have produced northwestward motion at 1-2 ms^{-1} on a Northern Hemispheric β-plane, despite zero background environmental steering flow (known as β-drift), and is the basis for the linear model considered here. The total motion of a TC can be considered as the vector sum of the advection by the background winds and the β-gyre propagation. Propagation is independent of the background flow to a first approximation. The concept from Figure 5 is utilized by the National Hurricane Center and implemented into their Beta and Advection Model for track forecasting (Marks, 1992).

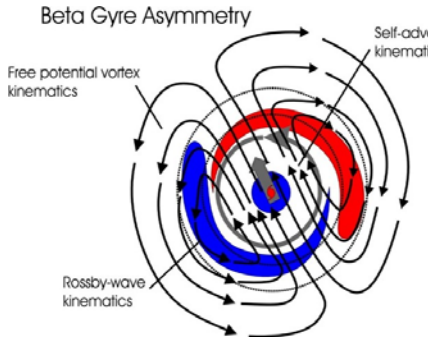

Figure 4. The impact of the β-effect on forming the β-gyres

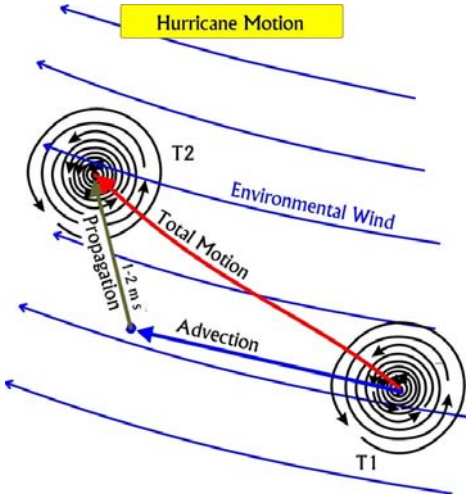

Figure 5. Vector motion to the WNW

VORTEX ROSSBY WAVES

General Structure and Propagation

Our study continues Cotto's (2012) work on Vortex Rossby Waves (VRWs); vorticity waves formed by the β-effect that propagate upon the radial gradient of mean vortex vorticity. In cyclonic vortices where the mean vorticity decreases outward (e.g., TCs), they propagate upstream so that their phase velocity with respect to the ground is slower than the mean swirling flow. Thus, VRWs are advected cyclonically downstream around the vortex. Two-dimensional Rossby waves in cylindrical coordinates are confined to a "passband" between zero frequency and the frequency of one-dimensional Rossby waves with the same tangential wavenumber. In a divergent context, vorticity stretching and advection can excite VRWs as can advection by the axisymmetric vortex of the gradient of planetary vorticity. Willoughby hypothesized that the β-gyres are VRW normal modes on completely cyclonic BND vortices (Montgomery & Kallenbach 1997).

DYNAMICS OF THE BND MODEL

Simulated Environment

Here, we revisit the work done in the late 1980s and 1990s, using a vortex-following 2-D model on a Northern Hemispheric β-plane and considers a BND vortex in a still environment initialized from asymmetry and rest. It is scaled to resemble a TC on a rotating spherical Earth. Time integration of the vorticity equation yields the asymmetric structure of the vortex, including a well-defined wavenumber-1 (WN1) asymmetry resulting from the displacement between the center of the rotation and the origin of the cylindrical coordinates. Periodically, the vortex is repositioned to remove the asymmetry and updates the motion inherited from previous computations. We use the simplest imaginable model exclusively on MATLAB that includes the essential rotational dynamics of the β-drift.

Vorticity Equation

A translating cylindrical coordinate system is a natural choice to represent a circular vortex (Figure 6). The variables used are v_0, mean tangential wind; r, radius; λ, azimuth angle reckoned cyclonically from north; u, radial perturbation wind component (positive outward); v, tangential perturbation wind component (positive cyclonically); ϕ, perturbation geopotential; and f_0, Coriolis parameter. We chose a fixed latitude (φ=20°N) to calculate f_0 because it is a typical location of TC genesis and to keep the model idealized. Vorticity equation derivation begins with the radial and tangential momentum equations (1a & 1b), where $\frac{\partial}{\partial t}+\frac{v_0}{r}\frac{\partial}{\partial \lambda}$ represents the linearized Lagrangian (individual) derivative; $\xi_0=\frac{2v_0}{r}+f_0$ is the inertial parameter; $\zeta_0=\frac{\partial v_0}{\partial r}+\frac{v_0}{r}+f_0$ is the mean-flow vorticity:

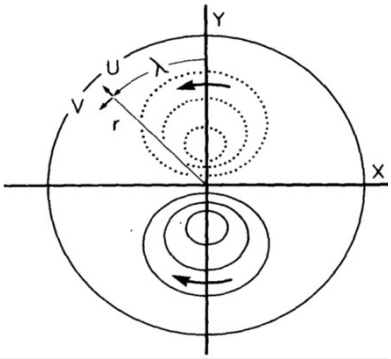

Figure 6. Cylindrical coordinate system (Willoughby 1987)

$$\frac{\partial u}{\partial t}+\frac{v_0}{r}\frac{\partial u}{\partial \lambda}-\left(\xi_0+\beta r\cos\lambda\right)v+\frac{\partial \phi}{\partial r}=0 \quad \text{(1a)},$$

$$\frac{\partial v}{\partial t}+\frac{v}{r}\frac{\partial v}{\partial \lambda}+\zeta_0 u+\frac{1}{r}\frac{\partial \phi}{\partial \lambda}=0 \quad \text{(1b)},$$

Cross-differentiating by taking $\frac{1}{r}\frac{\partial}{\partial \lambda}$ of (1a) and $\frac{\partial}{\partial r}+\frac{1}{r}$ of (1b) and subtracting effectively eliminates the geopotential terms and yields the vorticity equation:

$$\left(\frac{\partial}{\partial t}+\frac{v_0}{r}\frac{\partial}{\partial \lambda}\right)\left(\frac{\partial v}{\partial r}+\frac{v}{r}-\frac{1}{r}\frac{\partial u}{\partial \lambda}\right)+\zeta_0\left(\frac{\partial u}{\partial r}+\frac{u}{r}+\frac{1}{r}\frac{\partial v}{\partial r}\right)+u\frac{\partial \zeta_0}{\partial r}+\beta v\sin\lambda=0 \qquad (2).$$

The nondivergent nature of our model implies that the second term in (2) is zero.

Streamfunction

Since the flow is nondivergent, *u* and *v* can be represented with a streamfunction, $\psi(r,\lambda,t)$ such that, $u = -\frac{1}{r}\frac{\partial\psi}{\partial\lambda}$ and $v = \frac{\partial\psi}{\partial r}$. Therefore, (2) becomes:

$$\left(\frac{\partial}{\partial t} + \frac{v_0}{r}\frac{\partial}{\partial\lambda}\right)\left(\frac{\partial^2\psi}{\partial r^2} + \frac{1}{r}\frac{\partial\psi}{\partial r} + \frac{1}{r^2}\frac{\partial^2\psi}{\partial\lambda^2}\right) - \frac{1}{r}\frac{\partial\psi}{\partial\lambda}\frac{\partial\zeta_0}{\partial r} = \beta v\cos\lambda \qquad (3).$$

Solution Strategy

In moving coordinates, a convenient way to represent the wave solutions with tangential wavenumber, *n*, and apparent frequency, ω, is in terms of the real parts of the products of complex amplitudes such that, $\psi(r,\lambda,t) = \Psi(r)e^{i(\omega t - n\lambda)}$. The left side of equation (3) simplifies to obtain a dispersion relation for unforced free waves:

$$\left(\omega - \frac{nv_0}{r}\right)\left(\frac{d^2\Psi}{dr^2} + \frac{1}{r}\frac{d\Psi}{dr} + \frac{1}{r^2}\frac{d^2\Psi}{d\lambda^2}\right) + \left(\frac{n}{r}\frac{\partial\zeta_0}{\partial r}\right)\Psi = 0 \qquad (4),$$

Equation (4) may be solved for the Doppler-shifted frequency (Ω) and ω respectively:

$$\Omega = \left(\omega - \frac{nv_0}{r}\right) = -\frac{\left(\frac{n}{r}\frac{\partial\zeta_0}{\partial r}\right)\Psi}{\frac{d^2\Psi}{dr^2} + \frac{1}{r}\frac{d\Psi}{dr} + \frac{1}{r^2}\frac{d^2\Psi}{d\lambda^2}} \qquad (5),$$

$$\omega = \frac{nv_0}{r} - \frac{\left(\frac{n}{r}\frac{\partial \zeta_0}{\partial r}\right)\Psi}{\frac{d^2\Psi}{dr^2} + \frac{1}{r}\frac{d\Psi}{dr} + \frac{1}{r^2}\frac{d^2\Psi}{d\lambda^2}} \tag{6}.$$

Writing Ψ in terms of zero order Hankel functions $\Psi = H_0(k_r r)$, where k_r is the radial wavenumber allows us to solve for Ω to obtain a local dispersion relation for a nondivergent 1-D Rossby Wave.

$$\Omega = \left(\omega - \frac{nv_0}{r}\right) = -\frac{\frac{n}{r}\frac{\partial \zeta_0}{\partial r}}{k^2 + \frac{n^2}{r^2}} \tag{7}.$$

Since v_0 decreases with distance from the vortex center while r increases, v_0/r becomes smaller. The limits of wave propagation speed are dictated by k_r, which can be expressed as $2\pi/L_r$ (L_r is the local radial wavelength). The most negative Ω occurs when k_r is zero (e.g., L_r approaches negative infinity) which yields the fastest tangential wave propagation with respect to the mean wind. Consequently, (7) reduces to the dispersion relation for a 1-dimensional VRW. Vortex Rossby Wave "cutoff frequency" coincides with the maximum value of Ω at any given radius. When VRW's frequencies are Doppler-shifted to the cutoff frequency, wave reflection typically ensues. When Ω is zero, the waves become locally very short and continue to decrease in radial wavelength as they approach the critical radius. As k_r becomes large and $L_r \rightarrow 0$, radially propagating VRWs are absorbed at the VRW critical radius.

Lindzen-Kuo Solver

The definition of the vorticity reduces to a 2nd order differential equation with two endpoint boundary conditions. The Lindzen-Kuo algorithm (1969) solves the resulting Poisson equation for $\Psi(r)$ where boundary conditions are imposed at both ends of the domain. The equation is of the form $\frac{d^2\Psi}{dr^2} + g(r)\frac{d\Psi}{dr} + h(r)\Psi = F$, where g and h are constants and F is the forcing; ζ in this case. It can be written in finite difference form as,

$$\frac{\Psi_{n+1} + \Psi_{n-1} - 2\Psi_n}{\delta^2} + g_n\left(\frac{\Psi_{n+1} - \Psi_{n-1}}{2\delta r}\right) + h_n\Psi_n = F \tag{8},$$

where n is the radial index. Collecting like terms yields,

$$\left[\frac{1}{(\delta r)^2} - \frac{g}{2\delta r}\right]\Psi_{n-1} + \left[\frac{-2}{(\delta r)^2} + h\right]\Psi_n + \left[\frac{1}{(\delta r)^2} + \frac{g}{2\delta r}\right]\Psi_{n+1} = F \tag{9},$$

A_n, B_n, and C_n are defined to represent the terms inside the brackets so equation (9) becomes,

$$A_n\Psi_{n-1} + B_n\Psi_n + C_n\Psi_{n+1} = F \tag{10},$$

The solution for equation (10) is obtained by using the substitution:

$$\Psi_n = \alpha_n \Psi_{n+1} + \beta_n \qquad (11),$$

where $\alpha_n(r)$ and $\beta_n(r)$ are newly introduced variables.

Substituting (11) into (9) yields:

$$\alpha_n = \frac{-C_n}{A_n \alpha_{n-1} + B_n} \qquad \text{and} \qquad \beta_n = \frac{F - A_n \beta_{n-1}}{A_n \alpha_{n-1} + B_n} \qquad (12).$$

The arrays of $\alpha_1, \alpha_2, \ldots \alpha_{N-1}$ and $\beta_1, \beta_2, \ldots \beta_N$ are computed using (12) in an outward pass from n=0,…N, and then (10) is applied on an inward pass that starts with the outer boundary condition to compute $\Psi_{N-1}, \Psi_{N-2}, \ldots \Psi_1$.

LINEAR MODEL

Logic & Formulation

The linear model obtains solutions for the vorticity and streamfunction forced directly through *f*-advection by the mean swirling flow. Planetary and perturbation vorticity are advected by the axisymmetric flow and the perturbation radial flow advects axially symmetric mean vorticity. The model is based upon a time marching scheme to obtain the WN1 vorticity asymmetry. Solutions are semispectral with sinusoidal variation (WN1 only) in azimuth and finite-difference representation in radius and time. The domain extends to 4000 km radius with uniform 1 km resolution. In addition, the outer 500 km of the domain contains a "sponge ring" which, as the name suggests, absorbs waves through imposed strong Newtonian dissipation. Consequently, there is a prevention of the computation from being contaminated by outer boundary wave reflection. The linear model replicates linear β-gyre results (Willoughby 1992).

The general formulation for the linear model includes a movable mean vortex with fixed axially symmetric structure that is not allowed to change shape or intensity with time. The vortex obeys a Wood-White profile with specified maximum tangential wind (v_0=50 ms^{-1}), radius of maximum wind, RMW (25 km), and three power-law exponents that shape different portions of the velocity profile (Figure 7). The mean vortex is bounded in a similar manner as Willoughby's and resembles a TC at the threshold of Category-3 intensity. Beta gyres are hypothesized to be downstream propagating VRWs on the reversed peripheral mean vorticity gradient (Figure 8) confined in a band between zero and VRW cutoff frequency so that two waveguides

exist. The inner one supports propagation against (i.e., slower than) the cyclonic mean flow, while the outer has the waves propagate faster than the mean flow.

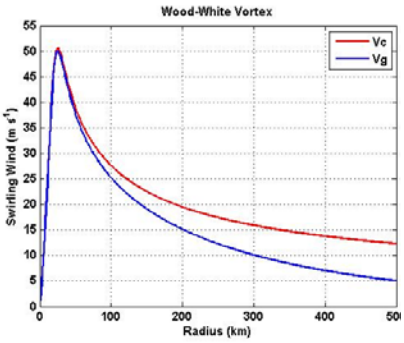

Figure 7. Wood-White cyclostrophic (V_c) & gradient (V_g) wind profile

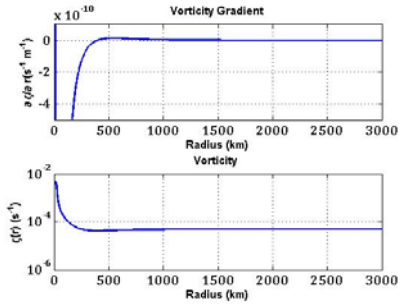

Figure 8. Radial vorticity and vorticity gradient

The model calculates the fixed vorticity and vorticity gradient, is initialized from zero perturbation amplitude and rest, marches the vorticity forward in 2.5-minute (150 s) time steps, and utilizes the Lindzen-Kuo solver to invert the vorticity to obtain the streamfunction. The new vorticity then becomes the input for the next time step. In addition, the vortex is tracked with a method known as "alpha (α) gyre closure" (Willoughby 1992). The α-gyres (sometimes referred to as psuedomodes) are apparent WN1 asymmetries that form near the RMW from mispositioning of the extrapolated vortex center, such that it is displaced from the origins of the coordinate system. To minimize the α-gyres, after each time step, the model finds the vortex centering error, relocates the center, and corrects the vorticity, streamfunction, and motion to the re-centered reference frame.

Vorticity Time Marching

Since our work is a time-marching problem, the derived nondivergent vorticity equation (2) is used to solve for the WN1 vorticity tendency:

$$\frac{\partial \zeta_1}{\partial t} = -\frac{v_0}{r}\frac{\partial \zeta_1}{\partial \lambda} - \left(u_1 - c_r\right)\frac{\partial \zeta_0}{\partial r} + \beta v_0 \sin\lambda \qquad (13).$$

The terms in (13) are: tangential vorticity advection (2nd term); radial vorticity advection including that because of the vortex motion, where $c_r = \mathrm{Re}\left\{-i\left(c_x + ic_y\right)e^{-i\lambda}\right\}$ is the translation speed in cylindrical coordinates (see Appendix 1); advection of the planetary vorticity gradient by the mean vortex. Unlike the earlier primitive equation model (Willoughby 1992) which ran for several minor time steps between relocations, the center is relocated after each time step. The numerics use leapfrog time-marching with an Asselin filter and typically runs for 10 simulated days or 240 hrs (equivalent to 2880 time steps).

Vortex Track, Speed, and Direction of Motion

The complete linear solution replicates the results of Willoughby (1992) with a predominantly NW track that accelerates throughout the simulation. During the 10-day period, the vortex moved a total distance of ~6000 km with an average speed of ~7 ms^{-1} and final speed of 14 ms^{-1} (Figure 9). The large distance traveled by the vortex in this model compared to Willoughby 1992 (~3800km) is attributed to nondivergence. The Poisson equation used here does not contain the Rossby radius term so that it yields a

larger streamfunction amplitude than the divergent model would with the same vorticity. In addition, the mean vortex direction of motion was mostly 325^0 because of the combined westward and poleward movement (Figure 10). An important note to consider is that the speed is sensitive to changes in the Newtonian damping time (normally 1 day^{-1} or 1/86400 s). Larger values yield a decreased acceleration.

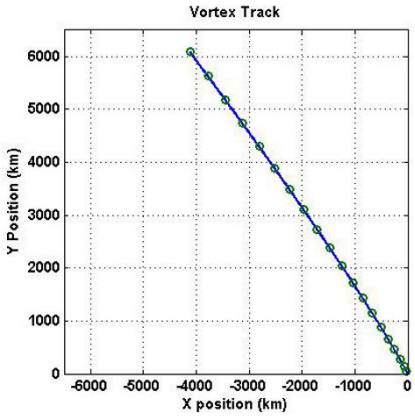

Figure 9. Vortex moves westward and poleward

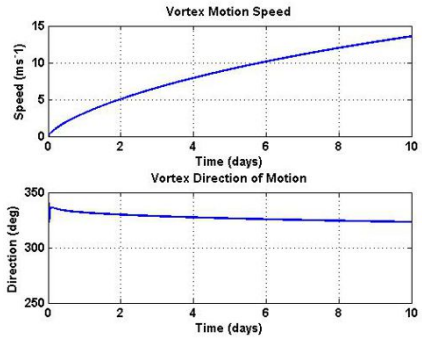

Figure 10. Unbounded acceleration in NW direction

Vorticity & Streamfunction

The vorticity field exhibits a trailing spiral pattern (akin to VRWs) with "filamentation" occurring around the center (Figure 11). The vorticity filaments wrap tightly around the vortex near the critical radius, where the frequencies are Doppler-shifted to zero. Vorticity waves' inward propagating energy gets absorbed at the critical radius where its wavelength becomes increasingly shorter. Conversely, waves that propagate outward approach the cutoff frequency and are reflected. The streamfunction field illustrates the β-gyres as dipoles of opposite polarity in the outer part of the vortex (Figure 12). Since the Lindzen-Kuo solver inverts the vorticity to calculate the

streamfunction, the streamfunction color scheme is reversed from the vorticity. Contours represent streamlines of the flow. The amplitude is proportional to the vortex speed and the flow between the asymmetries is consistent with a NW motion.

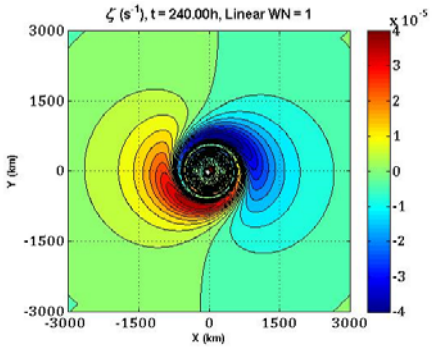

Figure 11. Linear vorticity field with trailing spirals and filamentation

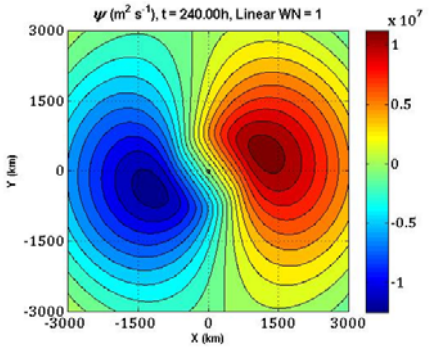

Figure 12. Linear streamfunction β-gyre asymmetries

Doppler-shifted Frequencies

Figure 13 depicts the variation of Doppler-shifted frequency for the β-gyres in the linear model. The VRWs in the outer waveguide have a very low (i.e., near zero) cyclonic frequency and propagate with a small group velocity in a narrow passband between zero frequency and the positive cutoff frequency. Beta forces the waves at zero frequency close to their resonance, allowing them to grow to large amplitude, therefore explaining the seemingly limitless accelerated motion in the linear model. The largest amplitude wave (for $\omega=1x10^{-6}$ s^{-1}) is confined to a radial interval between ~1100 km and 1700 km which includes the centers of the β-gyre WN1 asymmetries in Figure 12. The VRWs are weakly damped because the waveguide in which they are trapped is "leaky".

Initially inward propagating energy eventually reaches the critical radius where its vorticity becomes filamented and transferred to the mean flow. Initially outward propagating energy is ultimately reflected from the cutoff radius, then propagates inward and absorbed at the critical radius. Since the Doppler-shifted frequencies are so low, the radial group velocities are slow and dissipation by this process is gradual. Whether the VRWs represent a continuous spectrum or discrete normal modes is unclear; although the former interpretation seems more likely.

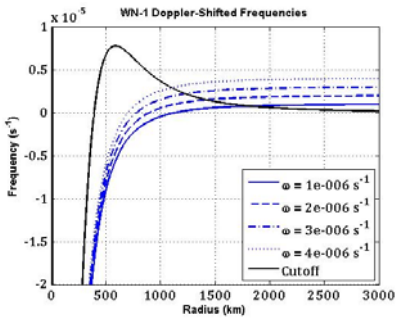

Figure 13. Doppler-shifted frequencies of the β-gyre waves

NONLINEAR MODEL

Logic & Formulation

The analogous nonlinear model includes wave-wave interactions between azimuthal wavenumbers by using a system of coupled, highly truncated partial differential equations that represent interaction between waves with azimuthal WN1 and WN2 semi-spectrally. That is, Fourier transformation in azimuth simplifies the system by yielding linear vorticity equations for WN1 and WN2 only, in which wave-wave interaction terms contain all of the nonlinearity. The wave-wave interactions of interest are: linear WN1 interacts with itself to force WN2 nonlinearly while WN1 interacts with WN2 to force WN1 nonlinearly (Figure 14).

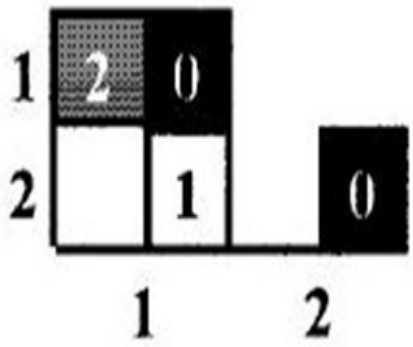

Figure 14. Wave-wave interaction diagram (Willoughby et al. 2000)

The formulation is similar to the linear model but the nonlinear version calculates linearly forced WN1, nonlinearly forced WN2, and nonlinearly forced WN1 vorticity and streamfunction. Computation of linear WN1 vorticity is exactly the same as in the linear model and yields the same results; apart from the effect of differing motion. The significant differences are in the WN2 and WN1 vorticity equations (with the nonlinear and wave-wave interaction terms), and provide a simplification of the earlier model (Willoughby 1994) inasmuch as nonlinearity limits vortex propagation relative to the linear model.

Vorticity Time Marching

The vorticity time marching method for the nonlinear model is the same as the linear model but includes nonlinear WN2 and WN1 vorticity tendency equations:

$$\frac{\partial \zeta_2}{\partial t} = -\frac{v_0}{r}\frac{\partial \zeta_2}{\partial \lambda} - u_2\frac{\partial \zeta_0}{\partial r} - \left(v_1 - c_\lambda\right)\left[\frac{1}{r}\frac{\partial \zeta_1}{\partial \lambda} - \beta \sin\lambda\right] - \left(u_1 - c_r\right)\left[\frac{\partial \zeta_1}{\partial r} + \beta\cos\lambda\right] \qquad (14).$$

The terms on the right-hand side of equation (14) are: linear tangential vorticity advection by the mean vortex, linear radial mean-vorticity advection by the perturbation flow, and nonlinear tangential and radial advection of perturbation and planetary vorticity. The nonlinear WN1 vorticity tendency equation is basically (13) with the additional terms (fourth to seventh) representing the forcing from β-effect and vortex motion:

$$\frac{\partial \zeta_1}{\partial t} = -\frac{v_0}{r}\frac{\partial \zeta_1}{\partial \lambda} - \left(u_1 - c_r\right)\frac{\partial \zeta_0}{\partial r} + \beta v_0 \sin\lambda - \left(\overline{v_1 - c_\lambda}\right)\frac{1}{r}\frac{\partial \zeta_2}{\partial \lambda} - v_2\left[\frac{1}{r}\frac{\overline{\partial \zeta_1}}{\partial \lambda} - \beta\sin\lambda\right]$$

$$- \left(\overline{u_1 - c_r}\right)\frac{\partial \zeta_2}{\partial r} - u_2\left[\frac{\overline{\partial \zeta_1}}{\partial r} + \beta\cos\lambda\right] \qquad (15).$$

The terms with the "over bar" symbol are complex conjugates (see Appendix 2). Equations (14) and (15) are marched forward in time using the semispectral algorithm with α-gyre closure (Willoughby 1994).

Vortex Track, Speed, and Direction of Motion

The nonlinear model results replicate Willoughby (1994) by significantly limiting the vortex translation speed. For the entire 10-day simulation, the vortex only travels ~2000 km (about 1/3 the distance traveled in the linear model), which is equivalent to an average speed slightly above 2 ms^{-1} (Figure 15). Most significantly, the translation speed asymptotes to just below 3 ms^{-1} early in the model run and maintains that fixed value until the end of the simulation. The direction of motion in Figure 16 is the same as the linear model (~325^0). The computed translation speed is slightly faster than the typical 1-2 ms^{-1} β-drift speed because of the BND formulation, and the larger basic vortex (3000 km) compared with the original model and nature. Outer circulation changes can affect the motion by changing the effective radius where the β-effect acts are excluded here.

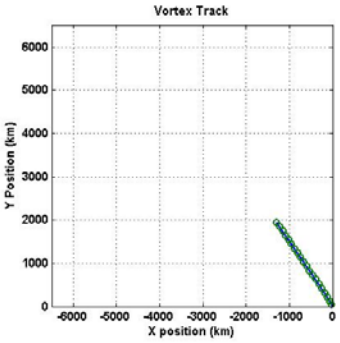

Figure 15. Limited vortex motion in the nonlinear model

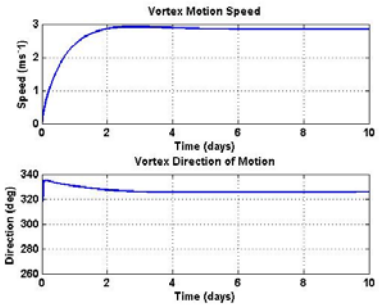

Figure 16. Vortex speed asymptotes after Day 2 in NW direction

Vorticity and Streamfunction of the Complete Solution

Solutions for vorticity and streamfunction are displayed as linear WN1, nonlinear WN2, and nonlinear WN1 asymmetries (Figures 17-21). The superposition of the accompanying results reduces the overall vortex translation speed shown earlier. Vorticity plots illustrate "trailing spiral" features and where filamentation is occurring near the critical radius (Figures 17 & 18). Analogous nonlinear streamfunction field contours exhibit asymmetries forced by wave-wave interaction. Interaction of WN1 with itself produces a “quadropole” structure that is typical when dealing with higher wavenumbers (Figure 20); WN3 for example would hypothetically yield a triple dipole structure. However, the most important and encouraging result stems from interaction of WN2 with WN1 to force nonlinear WN1 beta gyre-like asymmetries that are of opposite phase and lower amplitude to the linear gyres (Figure 21). Consequently, the ventilation flow between them is toward the southeast, thus counteracting the NW current of the linear asymmetries (Figure 19). Therefore, the nonlinearly-forced "anti-beta gyres" constitute the mechanism to which the nonlinear model controls the vortex speed.

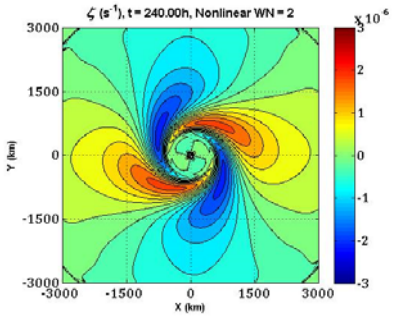

Figure 17. Nonlinearly-forced WN2 vorticity field

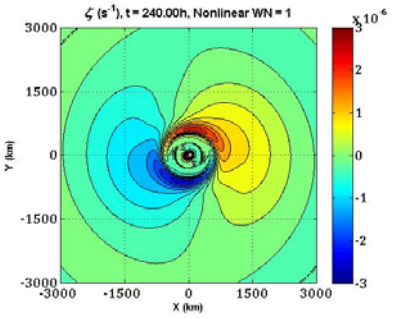

Figure 18. Nonlinearly-forced WN1 vorticity field

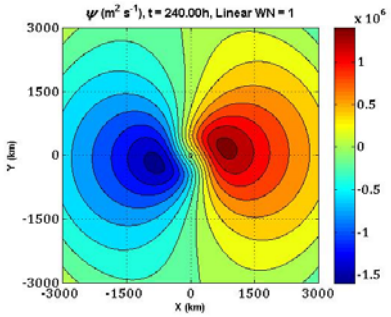

Figure 19. Linearly-forced WN1 β-gyre asymmetries

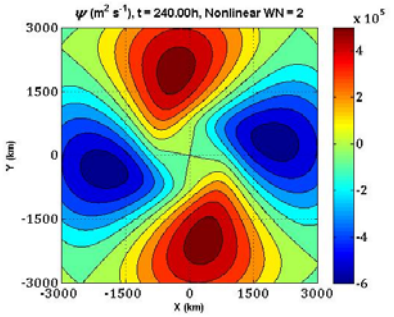

Figure 20. Nonlinearly-forced WN2 β-gyre double dipole asymmetries

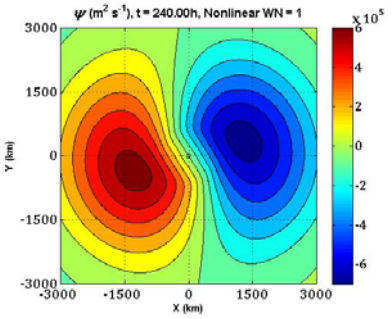

Figure 21. Nonlinearly-forced WN1 anti-β gyre asymmetries

STEADY STATE MODEL

Logic & Formulation

The predecessor of the original time-domain simulation was a frequency-domain model (Willoughby 1987) that attempted to simulate steady linear motion of a shallow-water (H=4 km) vortex on a β-plane. The model diagnosed the streamfunction, velocity potential, and geopotential at a specified frequency using the vorticity, divergence, and mass continuity equations. An unrealistically fast poleward and westward motion was produced and first prompted the hypothesis of a normal mode that is excited resonantly by the β-effect. Significance of nonlinear processes became apparent thereafter.

Here, the logic of his approach is explored in a BND context to gain insight into the β-gyres' dynamics. The frequency-domain model simulates for a single Fourier component at a specified frequency. The β-effect forcing is at zero frequency, but here, it has the same structure and rotates with a specified frequency, as the forthcoming streamfunction results will show. The domain is an annulus that excludes the immediate area around the origin thus, preventing growth of the α-gyre asymmetry from vortex motion. Steady state method exhibits a linear balance among forcing, tangential advection by the mean flow, and advection of mean vorticity by the radial perturbation flow.

The governing equation is the wavenumber-1 vorticity equation Fourier transformed in both time and azimuth (e.g., Cotto 2012) solved using Lindzen-Kuo algorithm for specified frequency, ω. Steady state method is simpler to work with and

provides an alternative to the time-marching linear problem. Exclusion of the domain center allows isolation of the β-gyres and the vortex here does not move.

Streamfunction & Resonance

The streamfunction was plotted for several specified positive and negative frequency values ranging from $1x10^{-4}$ s^{-1} to $-1x10^{-4}$ s^{-1} (Figures 22-27). Here, they are shown in descending order to illustrate how the β-gyres rotate with decreasing frequency by a magnitude of 10 in each frame (except from third to fourth). For a frequency of $1x10^{-4}$ s^{-1}, the β-gyre dipole is clearly evident with a north-south orientation (Figure 22). However, when we decrease the frequency to $1x10^{-5}$ s^{-1}, the asymmetries rotate slightly counter-clockwise such that their orientation is more northwest-southeast (Figure 23). The rotation pattern continues for the remaining four frames; Figure 24 produces the largest streamfunction amplitude, while the final frame (Figure 27) exhibits a complete 180^0 phase rotation from its positive counterpart. As before, the cool colors in Figures 22-27 correspond to cyclonic flow and vice-versa for 16-day dissipation. The maximum amplitude of the streamfunction is inversely proportional to the dissipation rate (i.e., 1/x), where x is an arbitrary number of days. Experimentation with different ω and dissipation values (e.g., 1-16 days) yields no apparent resonance for the imaginary part of the frequency.

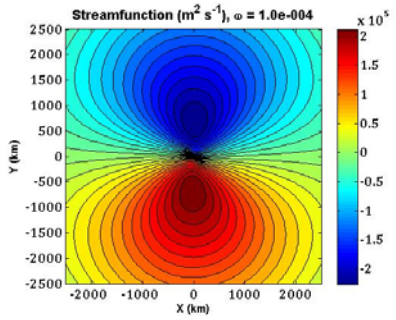

Figure 22. North-south oriented β-gyres for $\omega=1x10^{-4}$ s^{-1}

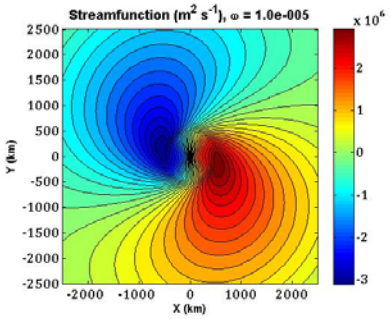

Figure 23. NW-SE oriented β-gyres for $\omega=1x10^{-5}$ s^{-1}

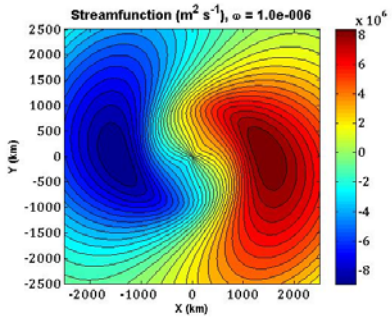

Figure 24. East-west oriented β-gyres for $\omega=1x10^{-6}$ s^{-1}

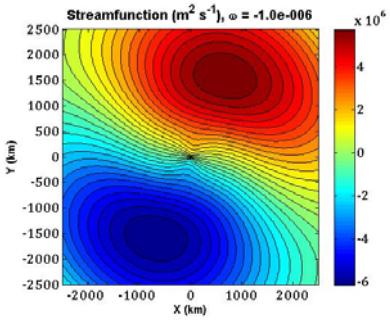

Figure 25. NE-SW oriented β-gyres for $\omega=-1x10^{-6}$ s^{-1}

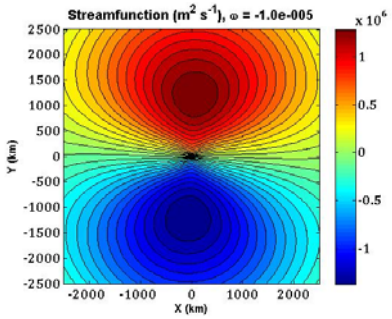

Figure 26. NNE-SSW oriented β-gyres for $\omega=-1x10^{-5}$ s^{-1}

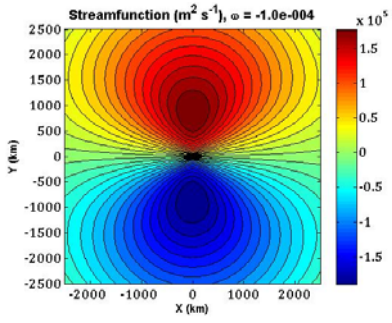

Figure 27. North-south oriented β-gyres for $\omega=-1x10^{-4}$ s^{-1}

Figure 28 illustrates the maximum streamfunction amplitude plotted as a function of frequency and clearly shows a peak in the resonant response at near-zero frequency. The streamfunction increases as the frequency becomes less negative and decreases with increasing positive frequency. Consequently, a phase reversal is apparent as the streamfunction amplitude goes through its maximum. In a non-resonant system, advection of vorticity by the mean vortex flow would be strongest on the east side, and the resulting vortex asymmetry most anticyclonic to the north. As the flow continued to circulate around, the streamfunction amplitude would become zero on the west side and acquire the most cyclonic vorticity passed south of the center. Beta gyre asymmetries would consequently form with a north-south orientation such that the ventilation flow would be easterly (270°). Conversely, the pattern of advection-induced gyres would reverse for a rotating source with frequency above the resonant frequency. Thus, the β-gyre phase in the original linear model (motion toward 325°) stems from the phase rotation across the resonant frequency at $\omega=1x10^{-6}$ s^{-1}.

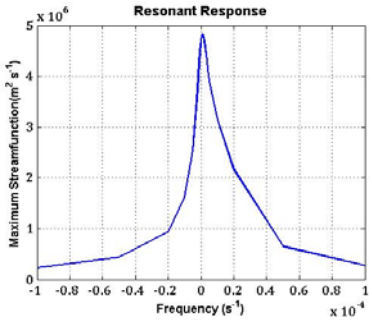

Figure 28. Resonant frequency at $\omega=1x10^{-6}$ s^{-1}

REINITIALIZATION OF THE LINEAR MODEL

Logic & Formulation

Another effective method for testing β-gyre normal mode theory is reinitialization of the linear model. The process involves rotating and scaling the β-gyres and then using them as initial conditions in an attempt to produce arbitrary motion on an *f*-plane to see if the result yields persistent motion. The working linear model was manually programmed to ask whether or not to reinitialize. Choosing "yes" will yield zero forcing at a specified time in the simulation followed by inputting a desired compass direction and day which should affect the vortex track. Selecting "no" on the other hand, allows the model to retain its forcing and will thus run normally. In the case shown here, we chose "yes", rotated the β-gyres 270^0 counter-clockwise, and turned off the β-effect at Day 5. Ideally, reinitialization should occur well after the β-gyres have had sufficient time to develop and establish themselves into well-defined WN1 asymmetries. In addition, we decided to extend the simulation to 15 days (360 hrs) to test the gyres' resilience under adverse conditions.

Vortex Track, Speed, and Direction of Motion

As in the original linear model, motion on a β-plane is a steady acceleration to the NW for the first 4 days but reinitialization 2000 km north of the starting point causes the vortex to turn westward. For the remainder of the simulation it follows a slowly cyclonically-curving track (Figure 29). The turn is forced by artificially imposing a 270^0 β-gyre rotation. By Day 10 (five days after β was turned off), the vortex speed decreases

fairly quickly but ultimately, the rate of deceleration slows and levels off. The initial motion toward 325^0 shifts abruptly to 270^0 when the gyres are rotated and β is suppressed (Figure 30). The gradual cyclonic curvature of the track is consistent with the very low (but nonzero) frequencies and slow (small radial group velocity) leaking of wave energy to the critical radius described earlier.

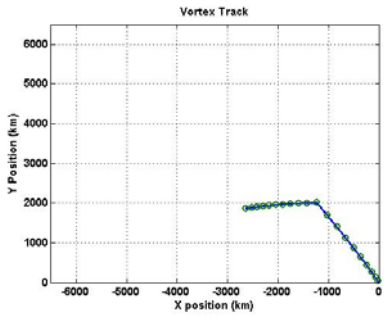

Figure 29. Vortex accelerates NW then curves cyclonically

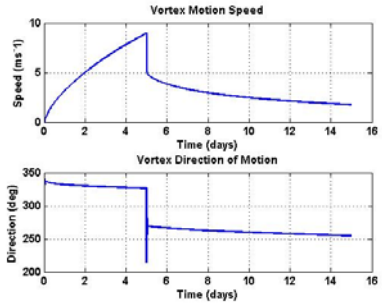

Figure 30. Pronounced shift in speed and direction after reinitialization

Streamfunction

Our working linear model initially runs on a β-plane until the forcing is turned off on Day 5 so that the remainder of the simulation operates on an *f*-plane. Figure 31 shows the streamfunction field at 360 hrs (i.e., 10 days after reinitialization) which clearly illustrates that the β-gyres' presence but with a north-south orientation such that the ventilation

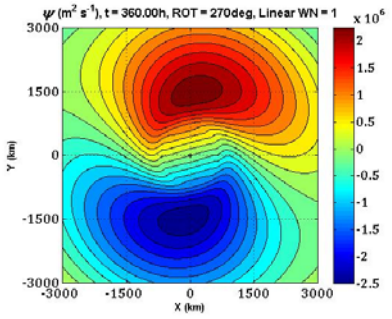

Figure 31. Reinitialized β-gyres rotated 270°

flow is toward the west-southwest. The asymmetries were rotated counter-clockwise 270^0 as we commanded the model to do and consequently force the vortex to shift to the cyclonic track mentioned earlier.

CONCLUSIONS

The BND vortex-following model allows us to focus on the rotational dynamics of TC motion initialized from rest in a quiescent environment on a Northern Hemispheric β-plane. Our linear results are consistent with the vortex-following linear primitive equation model of Willoughby (1992) as far as producing WN1 asymmetries with northeast-southwest orientation and a steadily accelerating NW speed. Indeed, β-gyres represent VRWs whose Doppler-shifted frequencies are confined to a frequency passband that corresponds to a narrow waveguide where they propagate downstream in the reversed vorticity gradient on the vortex periphery. Small Newtonian dissipation values were used; stronger values slow the motion. The analogous nonlinear results replicated earlier results (Willoughby 1994) inasmuch as wave-wave interactions limited the vortex translation speed to reasonable values. In addition, the isolation of nonlinearly forced anti β-gyres reveals a clear and readily understood mechanism for the reduced motion. Therefore, reproducing the unbounded linear and bounded nonlinear acceleration confirm earlier results. The radial variation Doppler-shifted frequencies illustrate that the β-gyres damp slowly with a VRW critical radius at the inner edge of the waveguide. Therefore, the β-gyres appear to represent a continuous spectrum of free VRWs confined in a narrow range of low cyclonic frequencies rather than discrete normal modes.

Two additional methods we utilized that helped us gain further insight into the β-gyres were steady state simulation and reinitialization. In the steady state model, the vorticity equation is forced at a specified frequency such that inner boundary conditions on an annular domain suppress the α-gyre asymmetries. Results produced β-gyre WN1

asymmetries that rotate counter-clockwise with decreasing frequency and a phase reversal occurs when the streamfunction passed its maximum amplitude. In reinitialization, the β-effect forcing is turned off at a specified simulated time and the vorticity field is scaled or reoriented. The vortex turns slowly in a cyclonic sense (for 270° phase rotation), consistent with the low cyclonic frequencies of VRWs in the outer waveguide. As vorticity leaks inward to the VRW critical radius (where they get absorbed) the β-gyres and motion decay fairly quickly before leveling off through the remainder of the simulation but do persist nonetheless. Furthermore, experimentation with other phase rotations (e.g., 90°, 180°, etc.) confirms that changing the orientation of the gyres alters the vortex track by producing any desired motion on an *f*-plane.

The existence of the outer waveguide is the key to understanding the β-gyres as free waves and permits propagation only in a narrow low-frequency passband. In a bounded vortex the passband encompasses only very low cyclonic frequencies, which correspond to a period of ~100 days. Resonance between the α-gyres at zero frequency and β-gyres at very low cyclonic frequencies is believed to be responsible for the unbounded linear acceleration. The nonlinear mechanism that limits acceleration is excitation of a free wave structure with the same shape, but opposite phase and reduced amplitude to the linearly forced β-gyres. Reinitialization on an *f*-plane produces very gradual cyclonic deflection of the vortex accompanied by steady decay as the wave energy propagates inward to the VRW critical radius at the proximal boundary of the waveguide. Consequently, the waveguide is "leaky" despite low radial group velocities since the waves become increasingly shorter such that radial wavenumber is large.

REFERENCES

Chan, Johnny C.L., and Williams, R.T., 1987: Analytical and Numerical Studies of the Beta-Effect in Tropical Cyclone Motion. Part I: Zero Mean Flow. *J. Atmos. Sci*., **44**, 1257-1265.

Chan, Johnny C.L., 2005: The Physics of Tropical Cyclone Motion: *Annu. Rev. Fluid Mech*., **37**, 99-128.

Cotto, Amaryllis, "Intermittently Forced Vortex Rossby Waves" (2012): *FIU Electronic Thesis and Dissertations*. Paper 553.

Holland, G.J., 1982: Tropical Cyclone Motion: Environmental Interaction Plus a Beta Effect. *J. Atmos. Sci*., **40**, 328-342.

Holland, G.J., 1983: Tropical Cyclone Motion: A Comparison of Theory and Observation. *J. Atmos. Sci*., **41**, 68-75.

Li, Xiaofan, Wang, Bin, 1993: Barotropic Dynamics of the Beta Gyres and Beta Drift. *J. Atmos. Sci.*, **51**, 746-756.

Lindzen, R.S., Kuo, H.L., 1969: A Reliable Method for the Numerical Integration of a Large Class of Ordinary and Partial Differential Equations. *Mon. Wea. Rev*., **97**, 732-734.

Marks, D.G., "The Beta and Advection Model for Tropical Cyclone Track Forecasts" (1992). *National Meteorological Center*. 4C.4.

Montgomery, M.T., Shapiro, L.J., 1992: A Three-Dimensional Balance Theory for Rapidly Rotating Vortices. *J. Atmos. Sci*., **50**, 3322-3335.

Montgomery, M.T., and Kallenbach R.J., 1997: A Theory for Vortex Rossby Waves and its Application to Spiral Bands and Intensity Changes in Hurricanes. *Quart. J. Roy. Meteor. Soc*., **123**, 435-465.

Montgomery, M.T., Moller, D.J., Nicklas, C.T., 1997: Linear & Nonlinear Vortex Motion in an Asymmetry Balance Shallow Water Model. *J. Atmos. Sci.*, **56**, 749-768.

Ritchie, E.A., Frank, W.M., 2006: Interactions between Simulated Tropical Cyclone and an Environment with a Variable Coriolis parameter. *Mon. Wea. Rev*., **135**, 1889-1905.

Willoughby, H.E., 1987: Linear Motion of a Shallow-Water, Barotropic Vortex. *J. Atmos. Sci*., **45**, 1906-1928.

Willoughby, H.E., 1990: Linear Normal Modes of a Moving, Shallow-Water Barotropic Vortex. *J. Atmos. Sci*., **47**, 2141-2148.

Willoughby, H.E., 1992*:* Linear Motion of a Shallow-Water Barotropic Vortex as an Initial-Value Problem. *J. Atmos. Sci*., **49**, 2015-2031.

Willoughby, H.E., 1994: Nonlinear Motion of a Shallow-Water Barotropic Vortex. *J. Atmos. Sci*., **51**, 3722-3744.

Willoughby, H.E., 1995: Normal-Mode Initialization of Barotropic Vortex Motion Models. *J. Atmos. Sci*., **52**, 4501-4514.

Willoughby, H.E., Jones, R.W., 2000: Nonlinear Motion of a Barotropic Vortex in Still Air and in an Environmental Zonal Flow. *J. Atmos. Sci*., **58**, 1907-1923.

Wood, Vincent T., Luther, White W., 2010: A New Parametric Model of Vortex Tangential-Wind Profiles: Development, Testing, and Verification. *J. Atmos. Sci.*, **68**, 990-1006.

Appendix 1- Complex representation of the moving cylindrical coordinate system

In the moving coordinates, a convenient way to represent the wavenumber 1 fields is in terms of the real parts of the products of complex amplitudes with $e^{-i\lambda}$ (Willoughby 1992). The combination of cylindrical and Cartesian coordinates yields the following relation:

$$(x - x_0) = -r\sin\lambda\,,$$

$$(y - y_0) = r\cos\lambda\,,$$

Such that $(x_0(t), y_0(t))$ are the vortex center coordinates. The Cartesian components for the vortex translation speed *C* is (c_x, c_y), where the complex representation of its amplitude is $-(c_x + ic_y)$. Applying some clever algebraic manipulation to the radial translation below yields a representation of the vortex motion in cylindrical components:

$$\begin{aligned} c_r = c_y\cos\lambda - c_x\sin\lambda &= \mathrm{Re}\{-i\cdot ic_y\cos\lambda + i\cdot ic_x\sin\lambda\} \\ &= \mathrm{Re}\{-i[ic_y\cos\lambda - ic_x\sin\lambda]\} \\ &= \mathrm{Re}\{-i[(c_x + ic_y)(\cos\lambda - i\sin\lambda)]\} \\ &= \mathrm{Re}\{iCe^{-i\lambda}\} \end{aligned}$$

Similarly for the tangential vortex translation we have,

$$
\begin{aligned}
c_\lambda = -c_x \cos\lambda - c_y \sin\lambda &= \mathrm{Re}\left\{ i \cdot ic_x \cos\lambda - (-i \cdot i) c_y \sin\lambda \right\} \\
&= \mathrm{Re}\left\{ -(c_x + ic_y)(\cos\lambda - i\sin\lambda) \right\} \\
&= \mathrm{Re}\left\{ Ce^{-i\lambda} \right\}
\end{aligned}
$$

Appendix 2- Complex conjugate terms in the nonlinear WN1 vorticity tendency equation

Some of the terms are complex conjugates that can be understood with the following expression:

$$\mathrm{Re}\left\{Ae^{-in\lambda}\right\}\mathrm{Re}\left\{Be^{-im\lambda}\right\} \quad \text{(I)},$$

Where A & B are arbitrary complex amplitudes and n & m are arbitrary tangential wavenumbers

$$\mathrm{Re}\left\{Ae^{-in\lambda}\right\} = \frac{1}{2}\left[Ae^{-in\lambda} + \overline{A}e^{in\lambda}\right] \quad \text{(II)},$$

Where $\overline{A}$ is the complex conjugate (similar for B). Applying (II) to (I) by using simple algebra and combining like terms yields this relation:

$$\frac{1}{2}\left[\mathrm{Re}\left\{ABe^{-i(n+m)\lambda}\right\} + \mathrm{Re}\left\{A\overline{B}e^{-i(n-m)\lambda}\right\}\right]$$